Reverberation mapping of a $z \sim 0.375$ active galactic nucleus

M.S Hlabathe[1,2]**, E. Romero-Colmenero**[1,3]**, S. M. Crawford**[1] **and LCO AGN Key collaboration**

[1]South African Astronomical Observatory, PO Box 9, Observatory, Cape Town, South Africa
[2]Astronomy Department, University of Cape Town, Private Bag X3, Rondebosch 7701, South Africa
[3]Southern African Large Telescope, PO Box 9, Observatory, Cape Town, South Africa

E-mail: `mh@saao.ac.za`

Abstract. Reverberation mapping is a technique that measures the time lag between the variable optical continuum from the accretion disk and the spectral line emission from the photo-ionized gas surrounding a super-massive black hole. The time lag is used to estimate the size of the emitting region, which is then assumed to be related to the mass of the super-massive black hole in the core of the active galactic nucleus. Using observations from the Southern African Large Telescope and Las Cumbres Observatory, we measure a time lag of $28.1^{+10.4}_{-27.7}$ days between the continuum and the broad Hβ feature in SDSS J143832.40+024804.1, an active galactic nucleus at $z = 0.375$. When combined with the velocity dispersion of the Hβ feature, we get a 1-sigma upper limit on the black hole mass to be $3.1 \times 10^8 \, \mathrm{M_\odot}$. These are preliminary results, extensive checks will be made to further refine the mass of the central black hole of SDSS J143832.40+024804.1.

1. Introduction

Broad emission lines are one of the prominent characteristics of type 1 Active Galactic Nuclei (AGN) [1]. Owing to the limitations of the resolution of present and even foreseeable future astronomical instruments, we have no way to resolve the broad emission line regions (BLRs) in AGN by direct observations. However, the structure of AGN on the smallest possible scales can still be probed through a process known as reverberation mapping [2, 3].

In AGN, stochastic continuum emission is produced from matter falling onto the accretion disk causing thermal instabilities within the disk. This continuum emission induces emission lines from gas clouds in the nearby (very few parsecs) BLR and more distant (tens of parsecs) narrow line region (NLR). Observationally, the emission lines in the BLR are broadened due to the high velocities and large Doppler shifts of the emitting clouds orbiting the central super-massive black hole (SMBH). Any variability in the continuum is 'echoed' by the gas clouds in the BLR after some time, with a time delay (τ) that depends on the light-travel time from the accretion disk to the BLR ($r = c\tau$). Combining τ and the velocity dispersion (σ_{line}) of the broad emission line, we can estimate the SMBH mass as $\mathrm{M_{SMBH}} = fr\sigma_{line}^2/G$, where f is a dimensionless factor to take into account geometric and orientation effects. Blandford & Mckee [2] were the first to establish reverberation mapping in trying to measure the black hole mass of an AGN.

Given the successful application of dynamical methods and reverberation mapping, there is strong evidence (both observational and theoretical) that there is a close connection between SMBH growth and galaxy evolution. Empirical relationships have been derived between the SMBH mass and the luminosity of the host galaxy bulge ($M_{BH} - L_{bulge}$), and between the SMBH mass and the spheroid velocity dispersion of the host galaxy bulge ($M_{BH} - \sigma_*$) for both nearby quiescent galaxies [4, 5] and distant AGN. To further understand the SMBH-galaxy connection, we need to compare and calibrate these correlations between local and distant samples. Unfortunately, due to observational difficulties associated with the reverberation mapping technique, there have been only ~ 50 SMBH mass estimates to date [6–10, e.g.]. The main difficulty lies in obtaining long monitoring campaigns with good signal-to-noise and cadence to ensure an accurate measurement of SMBH masses - poor reverberation mapping sampling leads to SMBH mass estimates with larger uncertainties [11].

In this paper, we estimate the SMBH mass in SDSS J143832.40+024804.1, an AGN at a redshift of $z \sim 0.375$, based on our Hβ observations. It is at this redshift that both Hβ and MgII(2800Å) can be observed at optical wavelengths, providing the unique opportunity to calibrate the SMBH mass estimates between these two samples (Hβ and MgII(2800Å)). This paper is the first step in a campaign that will also include MgII(2800Å) observations. We describe the observations and data analysis in Sect. 2, the measurement of the time lag in Sect. 3 and the estimate of the mass of the SMBH in Sect. 4.

2. Observations and Data analysis

We have obtained spectra from Southern African Large Telescope (SALT)[1] and continuum images for three AGN from several reverberation mapping campaigns as part of the Las Cumbres Observatory (LCO)[2] Key Project on Reverberation Mapping of AGN Accretion Flows [12]. In this paper we undertake the analysis of one of these AGN, SDSS J143832.40+024804.1, using only spectroscopic data from SALT. To carry out this analysis, continuum and emission line light curves are both derived from spectroscopy to estimate the lag and to measure the width of the emission line.

2.1. Spectroscopy

The spectra of SDSS J143832.40+024804.1 (ra = 14:38:32.40, dec = +02:48:04.20, J2000), were collected using SALT over 20 nights, from March 2015 to July 2016. In this work, we focus on the 16 spectra from 2015. The RSS spectrograph covers a wavelength range from $5200 - 8220$Å with a spectral resolution of $R \sim 1170$. Data reduction was handled using PySALT[3] [13]. The zSALT[4] pipeline currently incorporates PySALT and IRAF to fully automate the reduction steps which include bias subtraction, gain correction, cross-talk correction, amplifier mosaicing, and cosmic ray removal. The wavelength solution was calculated interactively using PySALT *specidentify*, a task to identify arc lines. The multiple spectral images taken on the same night were then median combined to produce one spectral image. The spatial center and the FWHM of SDSS J143832.40+024804.1 were used to extract the 1-D spectra. Flux calibration using spectrophotometric standard stars was done using *specsens*, a task defined in PySALT. The standard star calibration was then applied to spectra with the same observing configuration. Finally, telluric absorption was corrected for in our spectra.

Next, we flux calibrated our spectra based on the flux of the narrow emission line [O III] $\lambda 5008$Å, so that there is constant flux of [O III] $\lambda 5008$Å from one spectrum to the next.

[1] https://www.salt.ac.za
[2] https://lco.global
[3] http://pysalt.salt.ac.za/
[4] https://github.com/crawfordsm/zSALT

This is because we assumed the [O III] $\lambda5008$Å line not to be variable in the timescale of our monitoring campaign: the light travel time across the NLR is large (of the order of years) and the recombination time is also large (order of years), so for any short-term variability (few weeks to months), [O III] $\lambda5008$Å flux is essentially constant [14]. This process was accomplished by first, selecting the high signal-to-noise spectrum from 2015-03-03 as our reference spectrum. We then fitted the [O III] $\lambda5008$Å line in each individual spectrum, measuring its flux and rescaling the entire spectrum based on the flux of our chosen reference spectrum. We then aligned our spectra using the centre of the [O III] $\lambda5008$Å line in the reference spectrum. From the [O III] $\lambda5008$Å line recalibrated spectra, we construct the mean spectrum for Year 1 (2015), which can be seen in Fig 1.
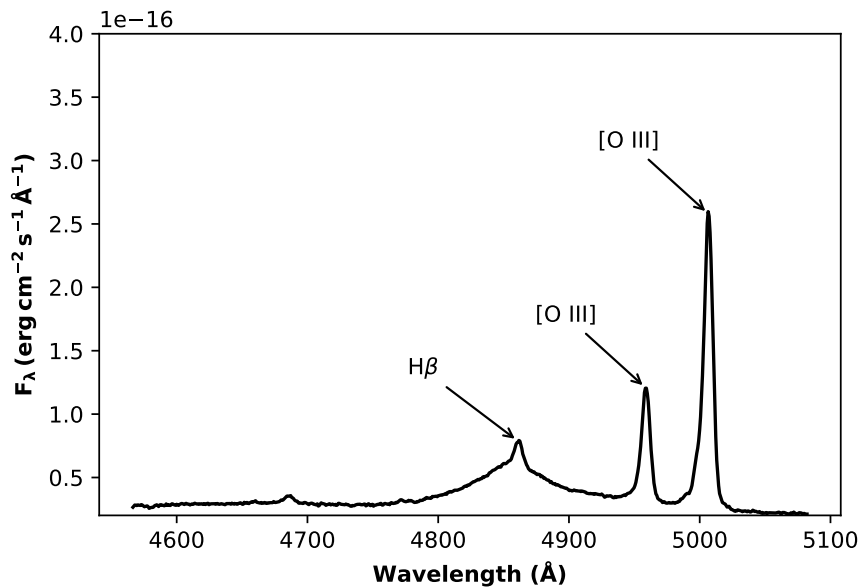

Figure 1. The mean spectrum of SDSS J143832.40+024804.1 for Year 1.

3. Time Lag Measurement

The spectroscopic continuum light curve at 5080Å and spectroscopic Hβ light curve are shown in Fig. 2. Both the Hβ light curve and continuum light curve at 5080Å were obtained through the use of *PREPSPEC* [15]. *PREPSPEC* again re-calibrated our [O III] $\lambda5008$Å pre-normalized spectra using the method described in [16]. After PREPSPEC is done with the flux calibration, it combines all individual spectra to produce mean and rms spectra. *PREPSPEC* then decomposes the spectra into various components, allowing for the measurements of the continuum and Hβ light curves. The Hβ light curve was obtained by integrating the flux after subtracting the best-fitting model components except for the broad Hβ model. The continuum light curve is generated by measuring flux at 5080Å in the rest frame. We then quantify the amplitude variability of the Hβ and continuum light curves as 0.061 ± 0.003 and 0.264 ± 0.004 respectively. The relatively small Hβ amplitude variability will limit the reliability of the time lag measurement [17].

3.1. Cross correlation

We employ the interpolation cross correlation function (ICCF, [18]) as implemented by [19] to cross correlate the Hβ and continuum light curve at 5080Å. The cross correlation function

(CCF) is measured twice. First by cross correlating the continuum with interpolated Hβ light curve, second by cross correlating the interpolated continuum with Hβ light curve. The final cross correlation is taken as the average of the two cross correlation results[5]. We define our cross correlation lag by the centroid τ_{cent} and the peak τ_{peak}. We report the lag of $\tau_{cent} = 28.1$ days and $\tau_{peak} = 29.0$ days (e.g., Fig 3).

To estimate the lag uncertainties, we employed the flux randomization and random subset selection method (FR/RSS, [20]). For each realization, N (same size as the original set) pairs of randomly selected measurements are drawn from the original dataset regardless of whether or not they have been previously selected. This results in some of the pairs being excluded and others being selected more than once. In the resulting set, redundant measurements are ignored which effectively reduces the set to typically 37% of the original set. Each measurement A_i from the drawn subset is modified by adding random Gaussian deviates based on the associated error α_i. Each drawn subset gives a cross-correlation series from which τ_{cent} and τ_{peak} are derived. Many realizations, in this case 3000, are used to build up a cross-correlation distribution which yields the median lag (τ_{cent} and τ_{peak}) and the 68.27% confidence interval. From the distribution, we obtained the uncertainties as $\tau_{cent} = 28.1^{+10.4}_{-27.7}$ days and $\tau_{peak} = 29.0^{+10.2}_{-32.0}$ days.
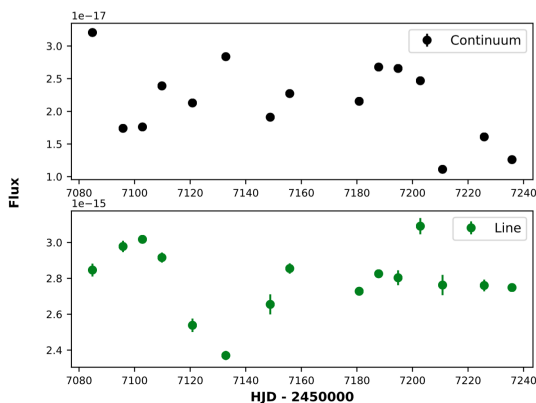

Figure 2. Continuum at 5080Å (top panel) and broad Hβ light curve (lower panel).
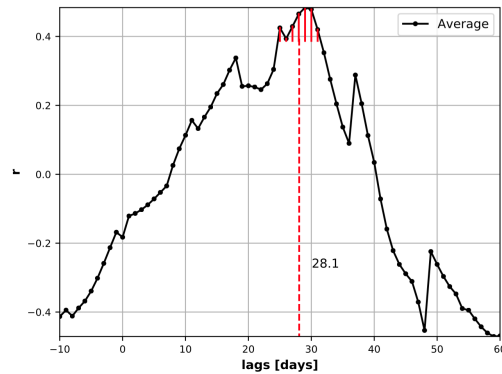

Figure 3. The CCF of Hβ and continuum light curves of SDSS J143832.40+024804.1 using only Year 1. The red dotted lines indicate all values above 80% threshold used to calculate τ_{cent}, yielding 28.1 days. We also record a τ_{peak} of 29.0 days. The lags are from -10 to 60 with the spacing of 1 day.

4. Black Hole Mass

To estimate the mass of the super-massive black hole, we need two parameters, the lag τ and the velocity dispersion of the emission line σ_{line}. σ_{line} is usually obtained from the rms spectra, the variable part of the emission line. Given that our rms spectra has a very weak Hβ variability and is dominated by residuals, we use the mean spectra instead. We construct the mean spectra by subtracting contributions from the narrow lines from each of the individual spectrum used to create the mean spectra. We used the fact that the ratio between [O III] $\lambda 5008$/[O III] $\lambda 4959$ is fixed at a value of 3, whereas the ratio Hβ_{narrow}/[O III] $\lambda 5008$ varied from spectrum to spectrum. Since we measured our Hβ line width from the mean spectra, we adopt the [21]

---

[5] https://github.com/hlabathems/iccf

calibration of the dimensionless factor for the line dispersion derived from the mean spectra, $f = 3.85$. Combining τ and σ_{line}, the black hole mass of $2.2^{+0.9}_{-2.2}\,(10^8\,\mathrm{M_\odot})$ was calculated. Due to under-sampling of our data, our measured time lag (and also the black hole mass) is consistent with zero. We also state that our light curves do not have enough data points and do not show significant variability to deduce beyond conviction that Hβ light curve does indeed lag the continuum light curve. Therefore the black hole mass we quote here of $3.1 \times 10^8\,\mathrm{M_\odot}$ is just an upper limit (1-sigma upper limit), and is based on the assumption that the two light curves are correlated.

Table 1. Reverberation mapping measurements of SDSS J143832.40+024804.1

AGN	Line	Amplitude variability	τ_{cent}	τ_{peak}	σ_{line}	FWHM	Mass
			(Days)	(Days)	(km s^{-1})	(km s^{-1})	(10^8 M$_\odot$)
1438	Hβ	0.061 ± 0.003	$28.1^{+10.4}_{-27.7}$	$29.0^{+10.2}_{-32.0}$	3235 ± 30	4974 ± 220	$2.2^{+0.9}_{-2.2}$

5. Summary

We used the spectra taken with SALT during 2015 campaign to measure the mass of the central black hole in SDSS J143832.40+024804.1. We then constructed Hβ and continuum light curves from the individual spectra using iraf, pysalt and prepspec, and we measure the Hβ lag to be $28.1^{+10.4}_{-27.7}$ days and $29.0^{+10.2}_{-32.0}$ days for τ_{cent} and τ_{peak}, respectively. We measure the velocity dispersion of the broad Hβ line to be $3235 \pm 30\,(\mathrm{km\ s^{-1}})$ from the mean spectra. Combining the Hβ lag (τ_{cent}) estimates with the velocity dispersion measurement obtained from the width of the Hβ emission line, we measure a mass for the central black hole of $2.2^{+0.9}_{-2.2}\,(10^8\,\mathrm{M_\odot})$. Our large uncertainty is primarily due to under-sampling of the light curve, and it will improve with the analysis of the full set of observations for SDSS J143832.40+024804.1. Future analysis and observations will allow calibrating our black hole mass by placing it in context to the most recent $M_{BH} - L_{bulge}$ and $M_{BH} - \sigma_*$ measurements.

References

[1] Seyfert C K 1943 *ApJ* **97** 28

[2] Blandford R D and McKee C F 1982 *ApJ* **255** 419–439

[3] Peterson B M 1993 *PASP* **105** 247–268

[4] Ferrarese L and Ford H 2005 *Space Sci. Rev.* **116** 523–624 (*Preprint* `astro-ph/0411247`)

[5] Kormendy J and Gebhardt K 2001 Supermassive black holes in galactic nuclei *20th Texas Symposium on relativistic astrophysics (American Institute of Physics Conference Series* vol 586) ed Wheeler J C and Martel H pp 363–381 (*Preprint* `astro-ph/0105230`)

[6] Wandel A, Peterson B M and Malkan M A 1999 *Astronomische Nachrichten* **320** 319

[7] Kaspi S, Smith P S, Netzer H, Maoz D, Jannuzi B T and Giveon U 2000 *ApJ* **533** 631–649 (*Preprint* `astro-ph/9911476`)

[8] Peterson B M, Ferrarese L, Gilbert K M, Kaspi S, Malkan M A, Maoz D, Merritt D, Netzer H, Onken C A, Pogge R W, Vestergaard M and Wandel A 2004 *ApJ* **613** 682–699 (*Preprint* `astro-ph/0407299`)

[9] Bentz M C, Walsh J L, Barth A J, Baliber N, Bennert V N, Canalizo G, Filippenko A V, Ganeshalingam M, Gates E L, Greene J E, Hidas M G, Hiner K D, Lee N, Li W, Malkan M A, Minezaki T, Sakata Y, Serduke F J D, Silverman J M, Steele T N, Stern D, Street R A, Thornton C E, Treu T, Wang X, Woo J H and Yoshii Y 2009 *ApJ* **705** 199–217 (*Preprint* `0908.0003`)

[10] Denney K D, Peterson B M, Dietrich M, Vestergaard M and Bentz M C 2009 *ApJ* **692** 246–264 (*Preprint* `0810.3234`)

[11] Park D, Woo J H, Treu T, Barth A J, Bentz M C, Bennert V N, Canalizo G, Filippenko A V, Gates E, Greene J E, Malkan M A and Walsh J 2012 *ApJ* **747** 30 (*Preprint* `1111.6604`)

[12] Valenti S, Sand D J, Barth A J, Horne K, Treu T, Raganit L, Boroson T, Crawford S, Pancoast A, Pei L, Romero-Colmenero E, Villforth C and Winkler H 2015 *ApJ* **813** L36 (*Preprint* `1510.07329`)

[13] Crawford S M, Still M, Schellart P, Balona L, Buckley D A H, Dugmore G, Gulbis A A S, Kniazev A, Kotze M, Loaring N, Nordsieck K H, Pickering T E, Potter S, Romero Colmenero E, Vaisanen P, Williams T and Zietsman E 2010 PySALT: the SALT science pipeline *Observatory Operations: Strategies, Processes, and Systems III* (*Proc. SPIE* vol 7737) p 773725

[14] Peterson B M 2009 *Active galactic nuclei* p 138

[15] Shen Y, Horne K, Grier C J, Peterson B M, Denney K D, Trump J R, Sun M, Brandt W N, Kochanek C S, Dawson K S, Green P J, Greene J E, Hall P B, Ho L C, Jiang L, Kinemuchi K, McGreer I D, Petitjean P, Richards G T, Schneider D P, Strauss M A, Tao C, Wood-Vasey W M, Zu Y, Pan K, Bizyaev D, Ge J, Oravetz D and Simmons A 2016 *ApJ* **818** 30 (*Preprint* `1510.02802`)

[16] van Groningen E and Wanders I 1992 *PASP* **104** 700–703

[17] Peterson B M 2014 *Space Sci. Rev.* **183** 253–275

[18] Gaskell C M and Sparke L S 1986 *ApJ* **305** 175–186

[19] White R J and Peterson B M 1994 *PASP* **106** 879–889

[20] Peterson B M, Wanders I, Horne K, Collier S, Alexander T, Kaspi S and Maoz D 1998 *PASP* **110** 660–670 (*Preprint* `astro-ph/9802103`)

[21] Collin S, Kawaguchi T, Peterson B M and Vestergaard M 2006 *A&A* **456** 75–90 (*Preprint* `astro-ph/0603460`)